Multiple steady states and dark states induced by nonlocal dissipation in a double quantum dot

Jianye Wei,[1,*] Hao Geng,[1,*] Wei Chen,[1,2,†] and D. Y. Xing[1,2]

[1]*National Laboratory of Solid State Microstructures and School of Physics, Nanjing University, Nanjing 210093, China*

[2]*Collaborative Innovation Center of Advanced Microstructures, Nanjing University, Nanjing 210093, China*

(Received 17 July 2022; revised 27 December 2022; accepted 5 January 2023; published 17 January 2023)

Both multiple steady states and dark states have potential applications in the quantum information processing in the presence of dissipation. Here, we propose to implement multiple steady states and dark states in a double quantum dot (DQD) system using quantum reservoir engineering. By coupling the DQD to shared reservoirs, multiple steady states of both four- and two-fold degeneracy can be achieved for specific parameters. It is proved that the occurrence of such multiple steady states is attributed to the strong symmetry of the Lindblad master equation. The multiple steady states can be well revealed by the occupation number of the DQD, which exhibits a discontinuity at the strong-symmetric points and changes drastically in the vicinities of these points. In the regime of unique steady state, the system can be stabilized to a pure state, dubbed dark state, with intact coherence in spite of the dissipation. Our work shows that a variety of novel steady states can be implemented in the DQD system, which paves the way for engineering multiple steady states and dark states in the DQD system.

DOI: 10.1103/PhysRevB.107.045416

I. INTRODUCTION

Coherent manipulation of a closed quantum system is implemented by controlling certain physical parameters so as to make the system evolve in a predesigned way via unitary evolution. However, when the system is coupled to a reservoir, its unitary evolution generally breaks down due to unavoidable gain and loss of particles as well as the decoherence effects. Surprisingly, apart from various negative effects, coupling with a reservoir also provides an alternative and effective way for the manipulation of the system, dubbed quantum reservoir engineering (QRE), i.e., controlling quantum states through proper environment designing [1]. It was demonstrated theoretically [2–5] and verified experimentally [6–9] that a properly designed dissipation can be used to prepare and stabilize correlated quantum many-body states. Moreover, dissipation can also be used to generate a nontrivial steady-state manifold with more than one eigenstates [10–12]. Such multiple steady states of open systems recently attracted much attention for its potential applications in quantum memory [13–15]. Specifically, quantum states can be encoded in the subspace spanned by the multiple steady states, which provides an effective scheme for autonomous quantum error correction [16–19].

In condensed matter physics, quantum dots (QDs) are well known for their high tunability and integrability [20–22], which makes them an ideal platform to implement various quantum devices [23,24]. State-of-the-art technologies allowed a coherent control [23,25,26] and readout [27–29] of quantum states in the QD systems. Among all candidates, the double quantum dot (DQD) systems are of particular interest because of their potential applications in nanotechnology and quantum information processing [30–33], which can be fabricated by the heterostructures of GaAs/AlGaAs [30]. Coherent manipulations of the DQD states were comprehensively studied, which can be achieved by a series of unitary operations induced by electric pulses imposed on the electrodes [23,26]. On the contrary, possible QRE on the DQD systems remains rarely explored although its high tunability strongly implies this feasibility, which may allow manipulations of the DQD states beyond the coherence time limit.

In this paper, we study QRE of the Liouvillian steady states in a DQD system coupled to separated and shared reservoirs [34]. The proposals using shared reservoirs to prepare nontrivial quantum states of photons and mechanical oscillators with steady-state entanglement and long-range coherence in optomechanical systems were widely studied [35–39]. In circuit quantum electrodynamics, the shared reservoir was proposed to stabilize entanglement between two remote qubits [9,40,41] or to control the dynamics of systems [42,43]. A recent study showed that even a single localized dissipative pairing interaction can be utilized to generate and stabilize complex many-body entangled states of fermions and qubits [44]. In this work, we focus on the new ingredient, the strong symmetry of the open DQD system, and uncover its relation to the occurrence of novel multiple steady states.

Under the framework of the Lindblad master equation, we show that the DQD exhibits rich steady states, which can be tuned by a variety of parameters, such as the coherence phases of the shared reservoirs, coupling to the separated reservoirs and the interdot hopping strength. Specifically, multiple steady states that possess four- or two-fold degeneracy can be implemented. We prove that the occurrence of such multiple steady states is attributed to the underlying strong symmetries of the system that arise for specific parameters. The multiple steady states can be well revealed by the

*These authors contributed equally to this work.

†Corresponding author: pchenweis@gmail.com

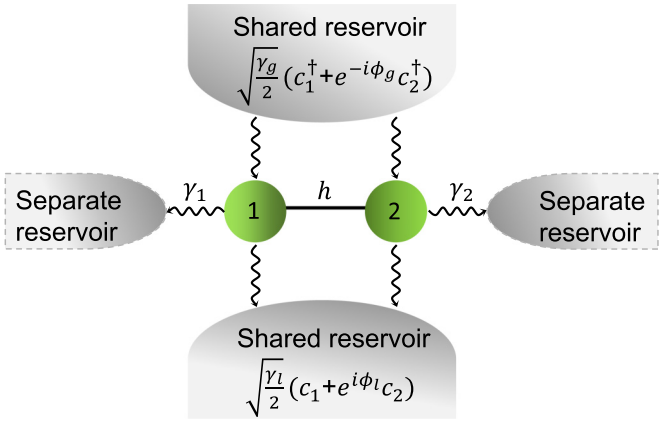

FIG. 1. The sketch of the setup. The DQD (1, 2) is coupled to the shared reservoirs that introduce both gain and loss with the respective rates γ_g and γ_l. Two separate reservoirs induce loss to the nearest dot with the rates $\gamma_{1,2}$. The interdot hopping of strength h is denoted by the solid line segment.

occupation number of the DQD in two aspects. First, the occupation number relies on its initial state and exhibits a discontinuity as the parameters deviate from the strong-symmetric points. Second, the occupation number changes drastically as the parameters vary in the vicinity of the strong-symmetric points. In addition to the multiple steady states, we also find that pure steady state or so-called dark state can also be achieved in the DQD system. The purity and coherence of such a dark state that depend on various physical parameters are discussed. Our work shows that QRE on the DQD quantum states can yield rich steady states, which may have interesting applications in quantum information processing.

The rest of the paper is organized as follows. In Sec. II, we describe the DQD system coupled to Markovian fermionic reservoirs by the Lindblad master equation. In Sec. III, we solve the Liouvillian spectrum and obtain the analytic expressions of the multiple steady states and discuss the effects of the relevant physical parameters. It is proved that the occurrence of the multiple steady states stems from the underlying strong symmetry of the system. In Sec. IV, we show that the multiple steady states can be manifested by the occupation number and the interdot current of the DQD. In Sec. V, we show that the dark state can also be implemented in certain parametric regions, of which the state coherence is discussed. Finally, we draw our main conclusion in Sec. VI.

II. MODEL

We consider a setup of the DQD coupled to several fermionic reservoirs, as shown in Fig. 1. Each dot is tuned to the Coulomb blockade regime such that only a single energy level needs to be considered. Thus, the Hilbert space for the DQD is spanned by the basis vectors $|00\rangle, |10\rangle, |01\rangle, |11\rangle$, where $|0\rangle$ and $|1\rangle$ represent the unoccupied and occupied states, respectively. Under the Born-Markov approximation, the dissipative dynamics of the density matrix $\rho(t)$ of the DQD can be described by the Lindblad master equation [45] (hereafter we set $\hbar = 1$)

$$\frac{d\rho}{dt} = -i[H, \rho] + \mathcal{D}[\rho] \equiv \mathcal{L}[\rho], \tag{1}$$

where $H = h(c_1^\dagger c_2 + \text{H.c.})$ is the interdot hopping with $c_{1,2}$ the fermion operators and h is the hopping strength. The on-site energy is set to zero without loss of generality. The dissipator is expressed as $\mathcal{D}[\rho] = \sum_\mu (2L_\mu \rho L_\mu^\dagger - \{L_\mu^\dagger L_\mu, \rho\})$ with L_μ the quantum jump operator associated with dissipative channel induced by the fermionic reservoir labeled by μ. [.,.] and {., .} denote the commutator and the anticommutator, respectively. Formally, the dynamics of the system is governed by the Liouvillian superoperator $\mathcal{L}$ which maps one density matrix to another. This map preserves the trace and Hermiticity of the density matrix and generates completely positive dynamics of the quantum state.

Two types of fermionic reservoirs are introduced here, namely, the shared and separate reservoirs, which result in the nonlocal and local dissipations, respectively; see Fig. 1. The jump operators due to two shared reservoirs contain the fermion operators of both dots. Such coherent dissipations can be realized by coupling the DQD to a wire or a two-dimensional (2D) electron gas parallel to the structure [34]. We are interested in the regime in which one shared reservoir introduces nonlocal gain effect while the other leads to nonlocal loss. Specifically, the jump operator for the nonlocal gain is $L_g = \sqrt{\gamma_g/2}(c_1^\dagger + e^{-i\phi_g}c_2^\dagger)$ and that for the nonlocal loss reads $L_l = \sqrt{\gamma_l/2}(c_1 + e^{i\phi_l}c_2)$ [34]. The parameters $\gamma_{g/l}$ are the rates of the gain/loss and $\phi_{g/l}$ are the coherent phases during nonlocal coupling, which are determined by the specific coupling between the DQD and the shared reservoirs. For the two separate reservoirs, the jump operator is expressed by the fermion operator of a single dot as $L_{j=1,2} = \sqrt{\gamma_j/2}c_j$. In the following discussion, we choose an equal rate of loss, i.e., $\gamma_{1,2} = \gamma$ for the DQD. In this work, we are interested in the effect induced by the coherent dissipation, which requires the dephasing effect to be weak enough. Specifically, the jump operators for the dephasing effect are $L_{j=1,2}^{\text{dep}} = \sqrt{\gamma_j^{\text{dep}}/2}c_j^\dagger c_j$. It is assumed that the dephasing rate γ_j^{dep} is much smaller than other dissipation rates of the system and so can be neglected.

The dual map of Eq. (1) that describes the evolution of physical observable O is known as the adjoint master equation, which reads [46]

$$\frac{dO}{dt} = i[H, O] + \sum_\mu (2L_\mu^\dagger O L_\mu - \{L_\mu^\dagger L_\mu, O\}) \equiv \mathcal{L}^\dagger[O]. \tag{2}$$

III. LIOUVILLIAN SPECTRUM AND MULTIPLE STEADY STATES

Given that the Liouvillian is a superoperator, it is convenient to map it to a $N^2 \times N^2$ matrix with N is the dimension of the Hilbert space $\mathcal{H}$ of the DQD system. Accordingly, the density matrices are mapped to a column vectors in the Fock-Liouville space. The spectral decomposition of the Liouvillian superoperator $\mathcal{L}$ can be formally expressed as

$$\mathcal{L}[r_i] = \lambda_i r_i, \tag{3}$$

where r_i are the right eigenmatrices and λ_i are the corresponding eigenvalues. It can be proved that $\mathrm{Re}[\lambda_i] \leqslant 0$ holds true for all eigenvalues due to the completely positive map of the Liouvillian. The eigenmatrices can be normalized as $\mathrm{Tr}[r_i^\dagger r_i] = 1$ by using the Hilbert-Schmidt inner product. Meanwhile, the orthogonality condition usually breaks down, i.e., $\mathrm{Tr}[r_i^\dagger r_j] \neq 0$, because $\mathcal{L}$ is generally not Hermitian,.

We are interested in the steady states ρ_{ss} of the system, namely the eigenmatrices corresponding to the zero eigenvalue such that

$$\dot{\rho}_{ss} = \mathcal{L}[\rho_{ss}] = 0. \tag{4}$$

For a finite dissipative system, there must be at least one steady state that does not evolve with time [47,48]. There may also exist fixed points with pure imaginary eigenvalues, which are referred to as oscillating coherence and are solely governed by the Hamiltonian part of $\mathcal{L}$ [48]. From the Liouvillian spectra, one can define the Liouvillian gap by the largest nonzero eigenvalue ($\lambda_i^{\max} \neq 0$) as $\Lambda = -\mathrm{Re}[\lambda_i^{\max}]$, which determines the long-time dynamics of the system.

Spectral decomposition for the adjoint Liouvillian operator $\mathcal{L}^\dagger$ can be conducted in a similar way as

$$\mathcal{L}^\dagger[l_i] = \lambda_i^* l_i. \tag{5}$$

The left eigenmatrices l_i generally differ from the right ones r_i because $\mathcal{L}$ is not Hermitian in general. A useful property of the left and right eigenmatrices is that they can comprise the biorthogonal basis, which satisfy $\mathrm{Tr}[l_i^\dagger r_j] = \delta_{ij}$. Moreover, there is also a correspondence between the steady states and the conserved quantities J that satisfy $\dot{J} = \mathcal{L}^\dagger[J] = 0$ [14].

In most cases, a dissipative system possesses a unique steady state [49]. Interestingly, some particular scenarios with multiple steady states may also exist, which are attributed to certain weak or strong symmetries of the Lindblad master equation [13]. In the following, we show that multiple steady states can be achieved in the DQD through QRE, which are the main focus of this work. We first ignore the interdot hopping and then discuss its effect on the steady states. Due to the shared reservoirs, the two dots are not really insulated even if there is no direct hopping between them.

A. Without interdot hopping: $h = 0$

In the limit that both the interdot hopping and separate reservoirs are absent ($\gamma = 0$), real Liouvillian spectrum λ_i ($i = 0, \ldots, 5$) can be analytically solved as

$$\begin{aligned} &\lambda_0 = 0,\ 2\lambda_1^{(4)} = \lambda_2 = -2(\gamma_l + \gamma_g), \\ &2\lambda_{3,\pm}^{(2)} = \lambda_{4,\pm} = -(\gamma_l + \gamma_g) \pm Q, \\ &\lambda_{5,\pm}^{(2)} = -\tfrac{3}{2}(\gamma_l + \gamma_g) \pm \tfrac{1}{2}Q, \end{aligned} \tag{6}$$

where $Q = \sqrt{\gamma_g^2 + \gamma_l^2 + 2\gamma_g\gamma_l \cos\delta\phi}$ with $\delta\phi = \phi_g - \phi_l$ the phase difference and the superscripts denote the degree of degeneracy. One can see that the Liouvillian spectrum depend only on the phase difference $\delta\phi$ between the nonlocal gain and loss rather than their specific values $\phi_{g,l}$.

As $\delta\phi \neq 0$ with its value being restricted to $\delta\phi \in [-\pi, \pi)$, the system possesses a unique steady state with $\lambda_0 = 0$ in Eq. (6), with the corresponding density matrix expressed as

$$\rho_{ss}^{(0)} = r_0/\mathrm{Tr}[r_0] = \begin{pmatrix} A & 0 & 0 & 0 \\ 0 & 1/2 - A & B & 0 \\ 0 & B^* & 1/2 - A & 0 \\ 0 & 0 & 0 & A \end{pmatrix}, \tag{7}$$

in which $A = \gamma_l\gamma_g[1 + \cos\delta\phi]/[2(\gamma_l + \gamma_g)^2]$ and $B = e^{i\phi_l}(e^{i\delta\phi}\gamma_g - \gamma_l)/[2(\gamma_l + \gamma_g)]$. Interestingly, multiple steady states appear for $\delta\phi = 0$, which results in $\lambda_0 = \lambda_{3,+}^{(2)} = \lambda_{4,+} = 0$. It can be proved that the occurrence of such multiple steady states stems from the strong symmetry of the Lindblad master equation at $\delta\phi = 0$, i.e., there exists a conserved quantity J that commutes with the Hamiltonian H and all the jump operators L_μ, see the Appendix for details.

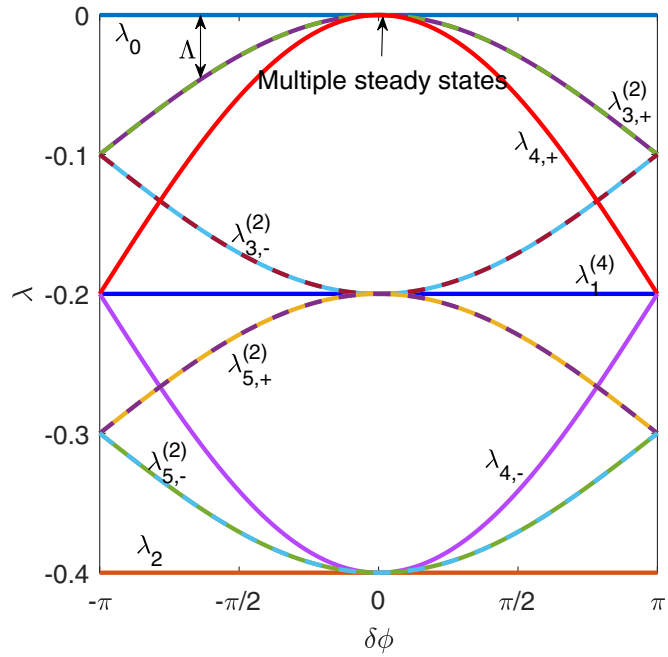

FIG. 2. The Liouvillian spectrum as a function of the phase difference between nonlocal gain and loss $\delta\phi = \phi_g - \phi_l$, where the double-headed arrows indicate the Liouvillian gap Λ. The relevant parameters are set as follows: $\gamma = 0$, $h = 0$, and $\gamma_l = \gamma_g = 0.1$.

In Fig. 2, we plot the Liouvillian spectrum as a function of $\delta\phi$, where the eigenvalues $\lambda_i = 0$ correspond to the steady states. Under the strong symmetry condition $\delta\phi = 0$, the spectrum possess a four-fold degeneracy and the Louvillian gap reaches its maximum, which corresponds to the minimum relaxation time of the system. A infinitesimal deviation of $\delta\phi$ from zero leads to a splitting of the multiple steady states and small gaps in between, which causes an extraordinarily long relaxation time of the system. Therefore, the Louvillian gap possesses a discontinuity at $\delta\phi = 0$. Far away from the strong symmetry point, the Louvillian gap reaches another local maximum at $\delta\phi = \pi$.

Here, we focus on the multiple steady states for $\delta\phi = 0$ and let $\phi_g = \phi_l = \phi$. The four eigenmatrices M_j ($j = 1, \ldots, 4$) describing the multiple steady states of the Liouvillian

superoperator can be obtained and orthogonalized as

$$M = C_1\left\{\begin{pmatrix}2\eta & 0 & 0 & 0\\ 0 & 1 & e^{i\phi} & 0\\ 0 & e^{-i\phi} & 1 & 0\\ 0 & 0 & 0 & 0\end{pmatrix},\begin{pmatrix}0 & 0 & 0 & 0\\ 0 & \eta & -\eta e^{i\phi} & 0\\ 0 & -\eta e^{-i\phi} & \eta & 0\\ 0 & 0 & 0 & 2\end{pmatrix},\begin{pmatrix}0 & -\eta & \eta e^{i\phi} & 0\\ -\eta & 0 & 0 & e^{i\phi}\\ \eta e^{-i\phi} & 0 & 0 & 1\\ 0 & e^{-i\phi} & 1 & 0\end{pmatrix},\right.$$
$$\left. i\begin{pmatrix}0 & -\eta & \eta e^{i\phi} & 0\\ \eta & 0 & 0 & e^{i\phi}\\ -\eta e^{-i\phi} & 0 & 0 & 1\\ 0 & -e^{-i\phi} & -1 & 0\end{pmatrix}\right\}, \tag{8}$$

where $C_1 = 1/(2\sqrt{1+\eta^2})$ is the normalization coefficient and $\eta = \gamma_l/\gamma_g$. The four matrices satisfy the orthonormalization condition $\mathrm{Tr}[M_i^\dagger M_j] = \delta_{ij}$. The eigenmatrices corresponding to the Liouvillian spectrum in Eq. (6) can be obtained by their linear combinations as

$$M_1' = \frac{M_1 - \eta M_2}{\sqrt{1+\eta^2}},\quad M_2' = \frac{M_2 + \eta M_1}{\sqrt{1+\eta^2}},\quad M_3' = \frac{M_3 - iM_4}{\sqrt{2}},\quad M_4' = \frac{M_3 + iM_4}{\sqrt{2}}. \tag{9}$$

Specifically, M_1' corresponds to the eigenvalue λ_0, which is identical to $\rho_{ss}^{(0)}$ for $\delta\phi = 0$; M_2' is the corresponding eigenmatrix of $\lambda_{4,+}$; M_3' and M_4' comprise a Hermitian conjugate pair which correspond to the eigenvalues $\lambda_{3,+}^{(2)}$ in Eq. (6).

Similarly, the conserved quantity can be obtained by solving the null space of $\mathcal{L}^\dagger$ according to $\mathcal{L}^\dagger[J] = 0$, which yields

$$J = C_2\left\{\begin{pmatrix}2 & 0 & 0 & 0\\ 0 & 1 & e^{i\phi} & 0\\ 0 & e^{-i\phi} & 1 & 0\\ 0 & 0 & 0 & 0\end{pmatrix},\begin{pmatrix}0 & 0 & 0 & 0\\ 0 & 1 & -e^{i\phi} & 0\\ 0 & -e^{-i\phi} & 1 & 0\\ 0 & 0 & 0 & 2\end{pmatrix},\begin{pmatrix}0 & -1 & e^{i\phi} & 0\\ -1 & 0 & 0 & e^{i\phi}\\ e^{-i\phi} & 0 & 0 & 1\\ 0 & e^{-i\phi} & 1 & 0\end{pmatrix},\right.$$
$$\left. i\begin{pmatrix}0 & -1 & e^{i\phi} & 0\\ 1 & 0 & 0 & e^{i\phi}\\ -e^{-i\phi} & 0 & 0 & 1\\ 0 & -e^{-i\phi} & -1 & 0\end{pmatrix}\right\}, \tag{10}$$

where the conserved quantities were normalized to assure the biorthogonality property, i.e., $\mathrm{Tr}[J_i^\dagger M_j] = \delta_{ij}$ with the coefficient $C_2 = \sqrt{(1+\eta^2)}/2(1+\eta)$. One can verify that the conserved quantities J_1 and J_2 are identical to Eq. (A3) for $\phi_l = \phi_g = \phi$.

For an arbitrary initial state ρ_{in}, the final steady state determined by the Liouvillian dynamics can be expressed by the multiple steady states in Eq. (8) and the conserved quantities in Eq. (10) as [14]

$$\rho_{ss} = \sum_{i=1}^{4} b_i M_i,\quad b_i = \mathrm{Tr}[J_i^\dagger \rho_{\mathrm{in}}]. \tag{11}$$

B. With interdot hopping: $h \neq 0$

Next, we consider more general cases with nonzero interdot hopping, where the strong symmetry is generally broken except for $\phi = 0, \pi$ (see the Appendix). In Figs. 3(a) and 3(b), we plot the real and imaginary parts of the highest four levels of the Liouvillian spectrum as a function of the interdot hopping for $\phi = \pi/4$. One can see that a finite interdot hopping lifts the degenerate multiple steady states by inducing a level splitting in both the real and imaginary parts of the spectrum.

Notably, the strong symmetry recovers for $\gamma = 0$ and $\phi = 0, \pi$. As a result, the degeneracy of Liouvillian spectrum is only partially lifted, which yields a zero eigenvalue with two-fold degeneracy as shown in Figs. 3(c) and 3(d). There are four fixed points with vanishing real part while only two of them are steady states with zero imaginary parts as well. It can be proved that the two-fold multiple steady states immune to the interdot hopping are the same as the first two steady states M_1 and M_2 in Eq. (8). The other two fixed points possess purely imaginary eigenvalues ih and $-ih$, which correspond to the eigenmatrices M_3' and M_4' in Eq. (9), respectively.

In the presence of strong symmetry, the final steady state can still be expressed by Eq. (11) with the same $b_{1,2}$ while different coefficients $b_{3,4}$ modified as

$$b_{3,4} = e^{\pm iht}\mathrm{Tr}[J_{3,4}'^\dagger \rho_{\mathrm{in}}], \tag{12}$$

with "±" corresponding to the subscripts 3,4, respectively, and

$$J_3'^\dagger = (J_3 - J_4)/\sqrt{2},\quad J_4'^\dagger = (J_3 + J_4)/\sqrt{2}. \tag{13}$$

C. Effect of interdot Coulomb interaction

In real DQD systems, the interdot Coulomb interaction may exist, which can be described by the Hamiltonian

$$H_C = U\hat{n}_1\hat{n}_2, \tag{14}$$

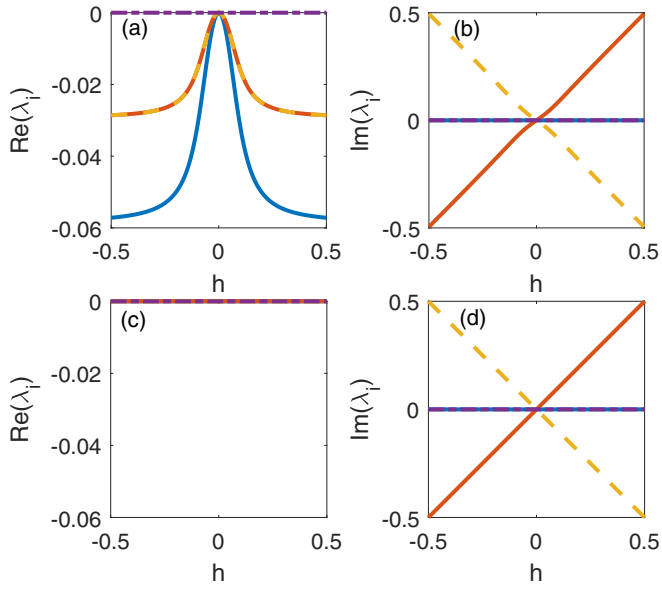

FIG. 3. The top four branches of the Liouvillian spectrum as a function of the interdot hopping, which contain both (a,c) the real components and (b,d) the imaginary components. The phase factors are set to (a,b) $\phi_l = \phi_g = \pi/4$ and (c,d) $\phi_l = \phi_g = \pi$, respectively. Other parameters are set as follows: $\gamma = 0$, $\gamma_l = \gamma_g = 0.1$.

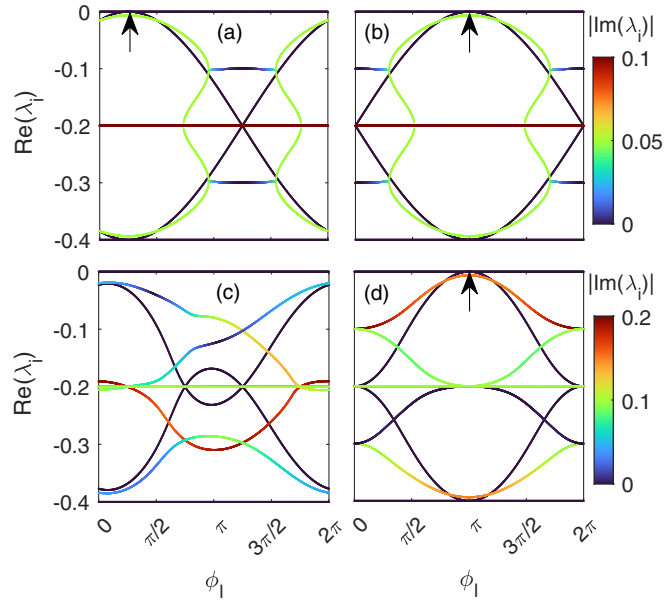

FIG. 4. The real part of Liouvillian spectrum as a function of ϕ_l, which contain both (a,b) the case for $h = 0$ and (c,d) the case for $h = 0.1$. The phase factors are set to (a,c) $\phi_g = \pi/4$ and (b,d) $\phi_g = \pi$, respectively. The arrows indicate the multiple steady states. The colormap depicts the modulus of the corresponding imaginary part. Other parameters are set as follows: $\gamma = 0$, $\gamma_l = \gamma_g = 0.1$, $U = 0.1$.

where $\hat{n}_j = c_j^\dagger c_j$ is the particle number operators, and U is the interaction strength. It can be verified that

$$[J, H_C] = 0 \tag{15}$$

holds true for arbitrary $\phi_{g,l}$. Thus, the Coulomb interaction does not break the strong symmetry at $\phi_l = \phi_g$ in the absence of local dissipation, dephasing, and interdot hopping and so the multiple steady states maintain. However, the degeneracy degree of the steady states is changed. In the presence of interdot Coulomb interaction, the Liouvillian spectrum becomes depends on the specific values of ϕ_l and ϕ_g, not only their difference. In Fig. 4, we plot the real part of Liouvillian spectrum as a function of ϕ_l for given ϕ_g. One can see clear steady-state degeneracy taking place at $\phi_l = \phi_g$ in the absence of interdot hopping, as indicated by the arrows in Fig. 4(a) and 4(b), where the real parts and imaginary parts (indicated by the colormap) of the spectrum are both vanished. For a finite interdot hopping, the steady-state degeneracy can only occur at $\phi_l = \phi_g = \pi$; see Figs. 4(c) and 4(d). It can be demonstrated that the steady states are of two-fold degeneracy with the eigenmatrices the same as the first two matrices in Eq. (8). Therefore, the interdot Coulomb interaction does not affect the physics around the strong symmetry points. Furthermore, we also verify that it will not affect the dark states for $\phi_g = \phi_l \pm \pi$ as well. In the next discussions, we will neglect the Coulomb interaction.

The multiple steady states that depend on the model parameters are summarized in Table I. It takes place only when the coupling between the DQD and the separate reservoirs is absent, i.e., $\gamma = 0$.

IV. OCCUPATION NUMBER AND CURRENT

Next, we discuss the manifestations of the steady states obtained in the last section by the occupation numbers and current in the DQD. We define the single-particle correlation function $\Delta_{ij}(t) = \mathrm{Tr}[c_i^\dagger c_j \rho(t)]$ whose time evolution can be derived by using Eq. (1), which yields [50]

$$\frac{d}{dt}\Delta(t) = X\Delta(t) + \Delta(t)X^\dagger + 2M_g, \tag{16}$$

where the damping matrix defined by $X = iH - (M_l + M_g)$ involves the contributions of the interdot hopping and the jump operators with

$$H = \begin{pmatrix} 0 & h \\ h & 0 \end{pmatrix}, \quad M_l = \frac{1}{2}\begin{pmatrix} \gamma_1 + \gamma_l & \gamma_l e^{i\phi_l} \\ \gamma_l e^{-i\phi_l} & \gamma_2 + \gamma_l \end{pmatrix}, \quad M_g = \frac{\gamma_g}{2}\begin{pmatrix} 1 & e^{-i\phi_g} \\ e^{i\phi_g} & 1 \end{pmatrix}. \tag{17}$$

TABLE I. Steady states for different parameters with $\gamma = 0$, where the abbreviation "MS(n)" denote the multiple steady states with n-fold degeneracies and "DS" denotes the dark state.

Parameters			Steady state
$h = 0$	$U = 0$	$\delta\phi = 0$	MS(4)
		$\delta\phi = \pm\pi$	DS
	$U \neq 0$	$\delta\phi = 0$	MS(2)
		$\delta\phi = \pm\pi$	DS
$h \neq 0$	Arbitrary U	$\phi_l = \phi_g = 0, \pi$	MS(2)
		$\delta\phi = \pm\pi$, with $\phi_l = 0, \pi$	DS

The diagonal elements of Eq. (16) give the time evolution of the occupation numbers $n_j = \Delta_{jj}$ as

$$\dot{n}_j = -(\gamma_j + \gamma_l)n_j + \gamma_g(1 - n_j) + I_{j\bar{j}} + I_d,$$
$$I_{j\bar{j}} = -ih(\Delta_{j\bar{j}} - \Delta_{\bar{j}j}), I_d = -\tfrac{1}{2}(\zeta\Delta_{12} + \zeta^*\Delta_{21}), \quad (18)$$

where j, $\bar{j}$ denote different dots and $\zeta = \gamma_l e^{i\phi_l} + \gamma_g e^{i\phi_g}$. The first term is the effective loss stemming from the anticommuting term of the dissipator $\mathcal{D}[\rho]$. The second term corresponds to the gain from the shared reservoir. The third term $I_{j\bar{j}}$ is the current flowing between the DQD caused by the coherent interdot hopping. Finally, the last term I_d are the interdot current induced by the dissipative coupling with the shared reservoir.

The interdot current $I_{j\bar{j}}$ does not affect the total electron number $n = n_1 + n_2$, which can be seen by noting that $I_{12} = -I_{21}$. Interestingly, the coupling to the shared reservoir gives rise to the other interdot current I_d that possesses the same formula as that due to coherent coupling. It takes place because the reservoir couples to the superposed state of both dots. Different from $I_{j\bar{j}}$, the current I_d has the same effect on both dots, which affect the total fermion number of the DQD. Here, we concentrate on the steady state, i.e., $\dot{n}_j^s = 0$ in Eq. (18). The steady occupation number of each dot can be expressed in terms of the currents and dissipation rates as

$$n_j^s = \frac{I_{j\bar{j}}^s + I_d^s + \gamma_g}{\gamma_l + \gamma_g + \gamma}, \quad (19)$$

with the superscript s denotes the values in the steady states.

A. Results for $h = 0$

We first consider the case with vanishing interdot hopping and $\gamma = 0$. In this case, $I_{j\bar{j}}^s = 0$ and the occupation numbers of both dots are equal. For a finite phase difference $\delta\phi \neq 0$, the system possesses a unique steady state of Eq. (7), from which the occupation number of each dot turns out to be a constant

$$n_j^s = \tfrac{1}{2}. \quad (20)$$

The DQD system possesses a strong symmetry for $\delta\phi = 0$ [cf. the Appendix], which gives rise to multiple steady states [cf. Table I]. As a result, the final steady state is a superposition of the multiple steady states, which strongly relies on the initial state of the system. Specifically, for an initial state

$$|\psi_0\rangle = \cos\alpha|10\rangle + \sin\alpha|01\rangle, \quad (21)$$

the corresponding steady states can be calculated by Eq. (11), which yields four coefficients $b_1 = C_2(1 + \cos\phi\sin 2\alpha)$, $b_2 = C_2(1 - \cos\phi\sin 2\alpha)$, and $b_3 = b_4 = 0$. The resultant occupation number of the DQD is then

$$n_j^s = \frac{1 - \cos\phi\sin 2\alpha}{4} + \frac{1}{2(1+\eta)}. \quad (22)$$

One can see that the occupation number generally relies on the coherent phase ϕ except for certain initial states with $\sin 2\alpha = 0$, as shown in Fig. 5(a). The phase ϕ determines the weights $p_i = b_i\mathrm{Tr}[M_i]$ of different steady states $\rho_i = M_i/\mathrm{Tr}[M_i]$. Specifically for $\alpha = \pi/4$, the minimum (maximum) of the occupation number take place at $\phi = 0$ ($\phi = \pi$), which corresponds to the final state ρ_1 (ρ_2). In the absence of nonlocal loss, i.e., $\eta = \gamma_l/\gamma_g = 0$, the maximum occupation number reaches its saturation value 1. In the opposite limit $\eta \to \infty$, the minimum occupation number becomes zero.

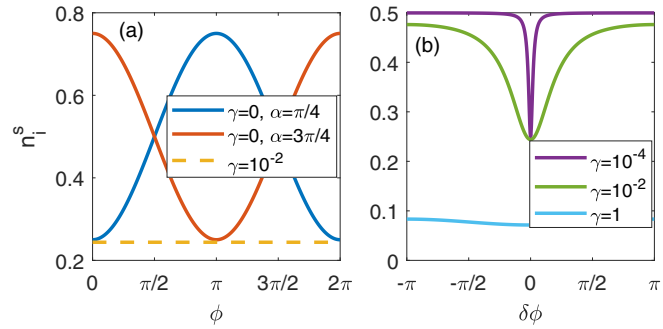

FIG. 5. (a) The occupation number of dot 1 (2) as a function of $\phi(=\phi_{g,l})$ for different initial states (solid lines) without local dissipation and the result with local dissipation (dashed line). (b) The occupation number as a function of the phase difference between the nonlocal gain and loss for various rates of the local dissipation. Other parameters are set as follows: $\gamma_l = \gamma_g = 0.1$, $h = 0$.

Finite local dissipations with $\gamma \neq 0$ break the strong symmetry regardless of $\delta\phi$ so that the system possesses a unique steady state independent of the initial state. For $\delta\phi = 0$, the unique steady state can be solved analytically as

$$\rho_{ss} = \frac{1}{2\eta + \gamma/\gamma_g + 2}\begin{pmatrix} 2\eta + \gamma/\gamma_g & 0 & 0 & 0 \\ 0 & 1 & e^{i\phi} & 0 \\ 0 & e^{-i\phi} & 1 & 0 \\ 0 & 0 & 0 & 0 \end{pmatrix}. \quad (23)$$

However, no concise expression of the steady state is available for $\delta\phi \neq 0$. One can solve the correlation function by Eq. (16) using the steady condition $\dot{\Delta}^s = 0$, which yields the Lyapunove equation

$$X\Delta^s + \Delta^s X^\dagger + 2M_g = 0. \quad (24)$$

The occupation number of the DQD can be obtained by its diagonal elements as

$$n_j^s = \Delta_{jj}^s = \left[\frac{1}{\gamma_g}\frac{\gamma(2\gamma_l + \gamma)}{\gamma_l(1 - \cos\delta\phi) + \gamma} + 2\right]^{-1}. \quad (25)$$

One can see that the occupation number depends only on the phase difference $\delta\phi$ between the nonlocal gain and loss. For a relatively small local dissipation, namely, $\gamma \ll \gamma_{l/g}$, where the strong symmetry is slightly broken, the occupation number is quite sensitive to $\delta\phi$ around its zero value; see the purple line in Fig. 5(b). For a finite $\delta\phi$, the occupation number is nearly a constant $n_j^s = 0.5$, independent of the phase difference. For $\delta\phi = 0$, the occupation number is $n_j^s = (2\eta + 2)^{-1}$, solely determined by the ratio between the rate of the nonlocal loss and gain. In the opposite limit $\gamma \gg \gamma_{l/g}$, the occupation number exhibits a weak dependence of $\delta\phi$, which is determined by the ratio between the local dissipation and nonlocal gain rates, namely, $n_i^s = (\gamma/\gamma_g + 2)^{-1}$; see the blue line in Fig. 5(b). The occupation number in the intermediate regime is plotted by the green line in Fig. 5(b), which exhibits a smooth dependence of $\delta\phi$.

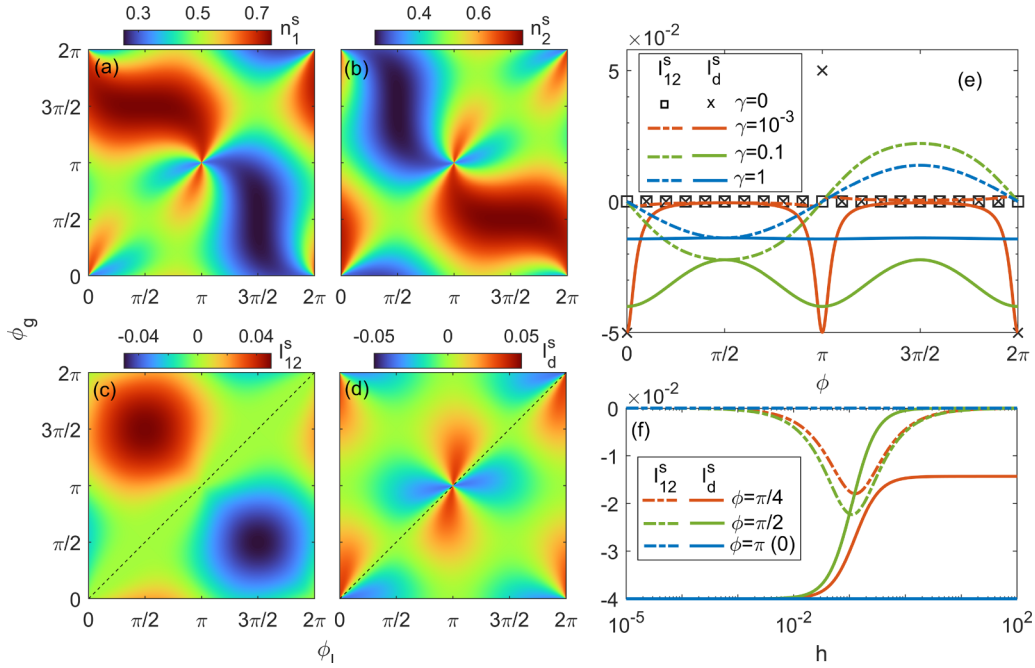

FIG. 6. The occupation numbers of (a) dot 1 and (b) dot 2, and the interdot current (c) I^s_{12} and (d) I^s_d vary with ϕ_g and ϕ_l with finite interdot hopping $h = 0.1$ and vanished local dissipation $\gamma = 0$. (e) I^s_{12} and I^s_d as functions of $\phi(= \phi_{g,l})$ for different rates of local dissipation. (f) The dependence of I^s_{12} and I^s_d on the interdot hopping for different ϕ with $\gamma = 0.1$. Other parameters are set as follows: $\gamma_l = \gamma_g = 0.1$.

B. Results for $h \neq 0$

As the interdot hopping is taken into account, the occupation numbers of the two dots rely on both $I_{j\bar{j}}$ and I_d [cf. Eq. (19)], which generally have different values. In Figs. 6(a) to 6(d), we numerically plot the occupation numbers $n^s_{1,2}$ and two kinds of current I^s_{12} and I^s_d with $\gamma = 0$. The results exhibit visible symmetric structures (with different values though) about the line $\phi_l = \phi_g$. Far away from the symmetric line, the occupation number is mainly determined by the interdot current. Specifically, both I^s_{12} and I^s_d have opposite values for the paired parametric points that are symmetric about the line $\phi_l = \phi_g$. Along the symmetric line, the steady-state density matrix is

$$\rho_{ss} = \frac{1}{(1+\eta)^2}\begin{pmatrix} \eta^2 & 0 & 0 & 0 \\ 0 & \eta & 0 & 0 \\ 0 & 0 & \eta & 0 \\ 0 & 0 & 0 & 1 \end{pmatrix}. \tag{26}$$

Accordingly, the currents I^s_{12} and I^s_d generally vanish, except that the latter possesses a finite value at the strong-symmetric points $\phi = 0, \pi$; see Fig. 6(e). In this case, there are two steady states M_1 and M_2 in Eq. (8), which dominate the occupations in the DQD. The initial state in Eq. (21) yields the same occupation number as that in Eq. (22). One can verify that the current I^s_d is not affected by the interdot hopping. Moreover, in the vicinity of the strong-symmetric points, I^s_d is drastically modified by the phases $\phi_{g,l}$; see Fig. 6(d). In the absence of strong symmetry, the occupation number of the DQD becomes $n^s_j = 1/(\eta + 1)$ along the line $\phi_g = \phi_l$ according to Eq. (19).

Next, we discuss the effect due to the local dissipation γ, which breaks the strong symmetry of the system and leads to a unique steady state. Nevertheless, the two types of currents can still be tuned by the phase ϕ; see Fig. 6(e). The interdot current I^s_{12} changes its sign at $\phi = 0, \pi$ for different local dissipation rate. Meanwhile, the current I_d is always negative. Interestingly, $I^s_{12} = I^s_d$ holds true for $\phi = \pi/2$ and $\gamma_{l/g} = h$, independent of the local dissipation; see Fig. 6(e). Moreover, I^s_{12} and I^s_d have different periods in ϕ, that is 2π for the former and π for the latter. Another notable feature of I_d is its high sensitivity to ϕ around $\phi = 0, \pi$ for a small local dissipation $\gamma = 10^{-3}$. It is a visible signature for the slight breaking of the strong symmetry of the system. For a relatively large local dissipation rate $\gamma = 0.1$, the magnitudes of I^s_{12} and I^s_d exhibit a negative correlation, showing competing effect. As the local dissipation rate increases further, the dissipative coupling current I^s_d tends to be independent of the phase.

The effects of the interdot hopping h on the currents are studied for various phase factors; see Fig. 6(f). Specifically, the unique steady state equals Eq. (23) for $\phi = 0, \pi$, so that the corresponding steady currents is independent on h as well. For $\phi \neq 0, \pi$, I^s_{12} is finite only within a certain parametric region of h while I^s_d exhibits a kink structure in the same region. For the special case $\phi = \pi/2$, I^s_d is completely suppressed by a large h.

V. DARK STATE AND ITS COHERENCE

Quantum coherence stemming from the principle of quantum superposition is the main resource of quantum computation and quantum information processing [51]. The interaction between a system with a reservoir usually leads to decoherence. Nevertheless, the dissipation may be beneficial for quantum coherence under some specific conditions, e.g., the bath-induced coherence [52,53], superradiance [54], and

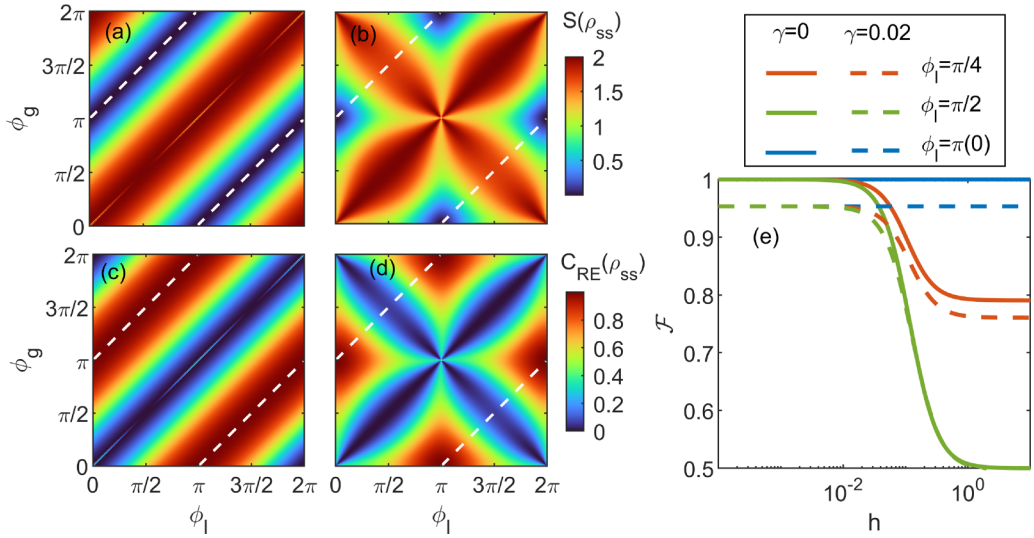

FIG. 7. The von Neumann entropy as a function of ϕ_g and ϕ_l for (a) $h = 0$ and (b) $h = 0.1$. The corresponding relative entropy is shown in (c) and (d). (e) The fidelity as a function of h for different ϕ_l and γ with $\phi_g = \phi_l + \pi$. Other parameters are set as follows: $\gamma_l = \gamma_g = 0.1$.

entanglement [4]. In this section, we study the steady-state coherence induced by the nonlocal dissipations. It turns out that the steady state superposed of $|10\rangle$ and $|01\rangle$ can preserve quantum coherence.

The quantum coherence can be measured by the relative entropy which defined as [55]

$$C_{\mathrm{RE}}(\rho) = S(\rho_{\mathrm{diag}}) - S(\rho), \tag{27}$$

where $S(\rho) = -\mathrm{Tr}[\rho \log_2 \rho]$ is the von Neumann entropy and ρ_{diag} is the matrix composed only of the diagonal elements of ρ. An important property of the relative entropy is that $C_{\mathrm{RE}}(\rho) = S(\rho_{\mathrm{diag}})$ holds true if and only if ρ is a pure state, which has vanishing von Neumann entropy $S(\rho) = 0$. In the context of quantum optics, such pure steady states $|D\rangle$ of an open quantum system are called dark states [2,56,57], which are the eigenstates of H and can be annihilated by all the quantum jump operators, namely, $L_{g/l}|D\rangle = 0$.

We show that dark states can be implemented in the DQD system in the absence of local dissipations. In Figs. 7(a) and 7(b), we plot the von Neumann entropy of the steady state as a function of $\phi_{g,l}$ for $h = 0$ and $h = 0.1$, respectively. In the absence of interdot hopping, the von Neumann entropy vanishes at $\phi_g = \phi_l \pm \pi$ as denoted by the dashed lines in Fig. 7(a). The zero von Neumann entropy manifests the dark state, which takes the explicit form of

$$|D\rangle = \frac{1}{\sqrt{2}}(|10\rangle - e^{-i\phi_l}|01\rangle). \tag{28}$$

The relaxation time from an initial state to the final dark state can be evaluated by $\tau_R \sim 2/(\gamma_l + \gamma_g)$, which is determined by the Liouvillian gap read from Eq. (6). It indicates that a rapid relaxation to the dark state can be implemented by high rates of the nonlocal gain and loss. A finite interdot hopping changes dramatically the pattern of the von Neumann entropy; see Fig. 7(b). It is noted that the von Neumann entropy remains zero at the points $(0, \pi)$ and $(\pi, 0)$, which corresponds to two dark states $|D\rangle = \frac{1}{\sqrt{2}}(|10\rangle \mp |01\rangle)$. For both cases, the dark states only depend on the phases $\phi_{g,l}$ rather than the specific rates $\gamma_{g,l}$ of the nonlocal gain and loss. The dependence of the dark states on relevant parameters are summarized in Table I.

The corresponding relative entropy $C_{\mathrm{RE}}(\rho_{ss})$ is shown in Figs. 7(c) and 7(d). It possesses the same pattern as that of the von Neumann entropy but with interchanged maximum and minimum, which can be inferred from its definition of Eq. (27). The maximal values of $C_{\mathrm{RE}}(\rho_{ss})$ correspond to the dark states, where the system possesses the strongest steady-state coherence. However, the saturation value of the relative entropy that is $C_{\mathrm{RE}} = \log_2 N = 2$ cannot be reached. In the strong-symmetric regime $\phi_l = \phi_g$, the von Neumann entropy and the steady-state coherence both depend on the initial state due to the multiple steady states.

In the presence of interdot hopping and local dissipation, the steady state ρ_{ss} of the system generally deviates from the dark states. Such a deviation can be quantified by the fidelity defined as [58]

$$\mathcal{F}(|D\rangle, \rho_{ss}) = \sqrt{\langle D|\rho_{ss}|D\rangle}. \tag{29}$$

For the specific case of $h = 0$ and $\gamma \neq 0$, the steady state is

$$\rho_{ss} = \frac{1}{\gamma/\gamma_g + 2}\begin{pmatrix} \gamma/\gamma_g & 0 & 0 & 0 \\ 0 & 1 & -e^{i\phi_l} & 0 \\ 0 & -e^{-i\phi_l} & 1 & 0 \\ 0 & 0 & 0 & 0 \end{pmatrix}, \tag{30}$$

and the corresponding fidelity is

$$\mathcal{F} = \left(1 + \frac{\gamma}{2\gamma_g}\right)^{-1/2}, \tag{31}$$

which depends only on the ratio between the rates of the local dissipation and the nonlocal gain. This formula can also be applied to the case of $h \neq 0$ and $\phi_l = 0, \pi$. The fidelity for more general cases is shown in Fig. 7(e). It is always independent of the interdot hopping for $\phi_l = 0, \pi$ (with $\delta\phi = \pi$). The lowest fidelity occurs at $\phi_l = \pi/2$, with $\mathcal{F} = 0.5$ for $\gamma = 0$, which exhibits weak dependence of the local dissipation as $h > 0.1$.

VI. CONCLUSION

To summarize, we studied the steady states of a DQD system engineered by shared fermionic reservoirs described using Lindblad master equation. This system exhibits rich steady states, involving both multiple steady states and dark states. We proved that the degenerate multiple steady states stem from the underlying strong symmetry of the open system. The multiple steady states are manifested as the parameter dependence of the occupation number. Our results have promising applications in the DQD-based quantum information processing, such as quantum error correction and state preparation against dissipations.

ACKNOWLEDGMENTS

This work was supported by the National Natural Science Foundation of China under Grants No. 12074172 (W.C.), No. 12222406 (W.C.), and No. 12174182 (D.Y.X.), Fundamental Research Funds for the Central Universities (W.C.), the startup grant at Nanjing University (W.C.), the State Key Program for Basic Researches of China under Grant No. 2021YFA1400403 (D.Y.X.), and the Excellent Programme at Nanjing University.

APPENDIX: SYMMETRY ANALYSIS

For a specific set of jump operators of Markovian dynamics described by the Lindblad master equation, if there is an operator J satisfying

$$[J, H] = [J, L_\alpha] = 0, \forall\alpha, \tag{A1}$$

then J is a conserved quantity, with

$$\dot{J} = \mathcal{L}^\dagger[J] = 0. \tag{A2}$$

In this case, there is a continuous symmetry $U(\theta) = \exp(i\theta J)$ (for real θ), such that $U(\theta)\mathcal{L}(\rho)U(\theta)^\dagger = \mathcal{L}[U(\theta)\rho U^\dagger(\theta)]$ for any state ρ of the system [13]. Then the system is said to have a strong symmetry, which assures the existence of the multiple steady states.

For the DQD system in our study, we focus on the operator

$$J = c_1^\dagger c_1 + c_2^\dagger c_2 - e^{i\phi_l} c_1^\dagger c_2 - e^{-i\phi_g} c_2^\dagger c_1, \tag{A3}$$

from which the existence of the strong symmetry can be inferred. Under some specific conditions, J becomes a conserved quantity. To see this, we calculate the following commutators:

$$\begin{aligned}
[J, H] &= h(e^{-i\phi_g} - e^{i\phi_l})(c_1^\dagger c_1 - c_2^\dagger c_2),\\
[J, L_l] &= \sqrt{\frac{\gamma_l}{2}}(e^{i(\phi_l-\phi_g)} - 1)c_1,\\
[J, L_g] &= \sqrt{\frac{\gamma_g}{2}}(1 - e^{i(\phi_l-\phi_g)})c_1^\dagger,\\
[J, L_1] &= \sqrt{\frac{\gamma}{2}}(-c_1 + e^{i\phi_l} c_2),\\
[J, L_2] &= \sqrt{\frac{\gamma}{2}}(-c_2 + e^{-i\phi_g} c_1).
\end{aligned} \tag{A4}$$

To achieve the strong symmetry, all four terms should be zero, which first requires the vanishing local dissipation $\gamma = 0$. In the absence of the interdot hopping, the first commutator is always zero. Therefore, the strong symmetry condition simply reduces to $\phi_l - \phi_g = 2m\pi$. According to Eq. (A2), the conserved quantities can be numerically obtained by solving the null space of $\mathcal{L}^\dagger$. For a finite interdot hopping, the strong symmetry requires both $\phi_l - \phi_g = 2m\pi$ and $\phi_l + \phi_g = 2n\pi$.

[1] J. F. Poyatos, J. I. Cirac, and P. Zoller, Phys. Rev. Lett. **77**, 4728 (1996).
[2] S. Diehl, A. Micheli, A. Kantian, B. Kraus, H. Büchler, and P. Zoller, Nat. Phys. **4**, 878 (2008).
[3] F. Verstraete, M. M. Wolf, and J. I. Cirac, Nat. Phys. **5**, 633 (2009).
[4] B. Kraus, H. P. Büchler, S. Diehl, A. Kantian, A. Micheli, and P. Zoller, Phys. Rev. A **78**, 042307 (2008).
[5] M. Müller, S. Diehl, G. Pupillo, and P. Zoller, Adv. At. Mol. Opt. Phys. **61**, 1 (2012).
[6] H. Krauter, C. A. Muschik, K. Jensen, W. Wasilewski, J. M. Petersen, J. I. Cirac, and E. S. Polzik, Phys. Rev. Lett. **107**, 080503 (2011).
[7] J. T. Barreiro, M. Müller, P. Schindler, D. Nigg, T. Monz, M. Chwalla, M. Hennrich, C. F. Roos, P. Zoller, and R. Blatt, Nature (London) **470**, 486 (2011).
[8] P. Schindler, M. Müller, D. Nigg, J. T. Barreiro, E. A. Martinez, M. Hennrich, T. Monz, S. Diehl, P. Zoller, and R. Blatt, Nat. Phys. **9**, 361 (2013).
[9] Y. Lin, J. Gaebler, F. Reiter, T. R. Tan, R. Bowler, A. Sørensen, D. Leibfried, and D. J. Wineland, Nature (London) **504**, 415 (2013).
[10] A. Beige, D. Braun, B. Tregenna, and P. L. Knight, Phys. Rev. Lett. **85**, 1762 (2000).
[11] P. Zanardi and L. Campos Venuti, Phys. Rev. Lett. **113**, 240406 (2014).
[12] Z. Leghtas, S. Touzard, I. M. Pop, A. Kou, B. Vlastakis, A. Petrenko, K. M. Sliwa, A. Narla, S. Shankar, M. J. Hatridge *et al.*, Science **347**, 853 (2015).
[13] B. Buča and T. Prosen, New J. Phys. **14**, 073007 (2012).
[14] V. V. Albert and L. Jiang, Phys. Rev. A **89**, 022118 (2014).
[15] D. Manzano and P. Hurtado, Adv. Phys. **67**, 1 (2018).
[16] F. Reiter, A. S. Sørensen, P. Zoller, and C. A. Muschik, Nat. Commun. **8**, 1822 (2017).
[17] E. Kapit, J. T. Chalker, and S. H. Simon, Phys. Rev. A **91**, 062324 (2015).
[18] J. Cohen and M. Mirrahimi, Phys. Rev. A **90**, 062344 (2014).
[19] S. Lieu, R. Belyansky, J. T. Young, R. Lundgren, V. V. Albert, and A. V. Gorshkov, Phys. Rev. Lett. **125**, 240405 (2020).
[20] L. Kouwenhoven and C. Marcus, Phys. World **11**, 35 (1998).
[21] L. P. Kouwenhoven, D. Austing, and S. Tarucha, Rep. Prog. Phys. **64**, 701 (2001).
[22] L. L. Sohn, L. P. Kouwenhoven, and G. Schön, *Mesoscopic Electron Transport* (Springer Science & Business Media, 2013).

[23] J. R. Petta, A. C. Johnson, J. M. Taylor, E. A. Laird, A. Yacoby, M. D. Lukin, C. M. Marcus, M. P. Hanson, and A. C. Gossard, Science **309**, 2180 (2005).
[24] R. Hanson, L. P. Kouwenhoven, J. R. Petta, S. Tarucha, and L. M. K. Vandersypen, Rev. Mod. Phys. **79**, 1217 (2007).
[25] T. Oosterkamp, T. Fujisawa, W. Van Der Wiel, K. Ishibashi, R. Hijman, S. Tarucha, and L. P. Kouwenhoven, Nature (London) **395**, 873 (1998).
[26] F. H. Koppens, C. Buizert, K.-J. Tielrooij, I. T. Vink, K. C. Nowack, T. Meunier, L. Kouwenhoven, and L. Vandersypen, Nature (London) **442**, 766 (2006).
[27] C. Barthel, D. J. Reilly, C. M. Marcus, M. P. Hanson, and A. C. Gossard, Phys. Rev. Lett. **103**, 160503 (2009).
[28] K. Nowack, M. Shafiei, M. Laforest, G. Prawiroatmodjo, L. Schreiber, C. Reichl, W. Wegscheider, and L. Vandersypen, Science **333**, 1269 (2011).
[29] K. D. Petersson, J. R. Petta, H. Lu, and A. C. Gossard, Phys. Rev. Lett. **105**, 246804 (2010).
[30] W. G. Van der Wiel, S. De Franceschi, J. M. Elzerman, T. Fujisawa, S. Tarucha, and L. P. Kouwenhoven, Rev. Mod. Phys. **75**, 1 (2002).
[31] J. M. Elzerman, R. Hanson, J. S. Greidanus, L. H. van Beveren, S. De Franceschi, L. M. K. Vandersypen, S. Tarucha, and L. P. Kouwenhoven, Phys. Rev. B **67**, 161308(R) (2003).
[32] J. M. Nichol, L. A. Orona, S. P. Harvey, S. Fallahi, G. C. Gardner, M. J. Manfra, and A. Yacoby, npj Quantum Inf. **3**, 3 (2017).
[33] T. Frey, P. J. Leek, M. Beck, A. Blais, T. Ihn, K. Ensslin, and A. Wallraff, Phys. Rev. Lett. **108**, 046807 (2012).
[34] D. Malz and A. Nunnenkamp, Phys. Rev. B **97**, 165308 (2018).
[35] A. Tomadin, S. Diehl, M. D. Lukin, P. Rabl, and P. Zoller, Phys. Rev. A **86**, 033821 (2012).
[36] H. Tan, G. Li, and P. Meystre, Phys. Rev. A **87**, 033829 (2013).
[37] M. J. Woolley and A. A. Clerk, Phys. Rev. A **89**, 063805 (2014).
[38] Y.-D. Wang and A. A. Clerk, Phys. Rev. Lett. **110**, 253601 (2013).
[39] C. Ockeloen-Korppi, E. Damskägg, J.-M. Pirkkalainen, M. Asjad, A. Clerk, F. Massel, M. Woolley, and M. Sillanpää, Nature (London) **556**, 478 (2018).
[40] S. Shankar, M. Hatridge, Z. Leghtas, K. Sliwa, A. Narla, U. Vool, S. M. Girvin, L. Frunzio, M. Mirrahimi, and M. H. Devoret, Nature (London) **504**, 419 (2013).
[41] L. C. G. Govia, A. Lingenfelter, and A. A. Clerk, Phys. Rev. Research **4**, 023010 (2022).
[42] J. Talukdar and D. Blume, Phys. Rev. A **105**, 063501 (2022).
[43] Z. Wang, T. Jaako, P. Kirton, and P. Rabl, Phys. Rev. Lett. **124**, 213601 (2020).
[44] A. Pocklington, Y.-X. Wang, Y. Yanay, and A. A. Clerk, Phys. Rev. B **105**, L140301 (2022).
[45] G. Lindblad, Commun. Math. Phys. **48**, 119 (1976).
[46] H.-P. Breuer and F. Petruccione, *The Theory of Open Quantum Systems* (Oxford University Press on Demand, Oxford, 2002).
[47] D. E. Evans and H. Hanche-Olsen, Preprint series: Pure mathematics http://urn.nb.no/URN:NBN:no-8076 (1977).
[48] B. Baumgartner and H. Narnhofer, J. Phys. A: Math. Theor. **41**, 395303 (2008).
[49] D. Nigro, J. Stat. Mech.: Theory Exp. (2019) 043202.
[50] F. Song, S. Yao, and Z. Wang, Phys. Rev. Lett. **123**, 170401 (2019).
[51] A. Streltsov, G. Adesso, and M. B. Plenio, Rev. Mod. Phys. **89**, 041003 (2017).
[52] C. L. Latune, I. Sinayskiy, and F. Petruccione, Quantum Sci. Technol. **4**, 025005 (2019).
[53] C. L. Latune, I. Sinayskiy, and F. Petruccione, Phys. Rev. A **99**, 052105 (2019).
[54] R. H. Dicke, Phys. Rev. **93**, 99 (1954).
[55] T. Baumgratz, M. Cramer, and M. B. Plenio, Phys. Rev. Lett. **113**, 140401 (2014).
[56] D. A. Lidar, I. L. Chuang, and K. B. Whaley, Phys. Rev. Lett. **81**, 2594 (1998).
[57] B. Buča, J. Tindall, and D. Jaksch, Nat. Commun. **10**, 1730 (2019).
[58] M. A. Nielsen and I. Chuang, *Quantum Computation and Quantum Information* (American Association of Physics Teachers, 2002).